This article has been accepted for publication in Tree physiology, published by Oxford University Press.The record is available online at: doi: 10.1093/treephys/tpv005

# The role of defoliation and root rot pathogen infection in driving the mode of drought-related physiological decline in Scots pine (*Pinus sylvestris* L.)

D. AGUADÉ[1,2,5], R. POYATOS[1], M. GÓMEZ[3], J. OLIVA[4] and J. MARTÍNEZ-VILALTA[1,2]

[1] CREAF, Cerdanyola del Vallès E-08193 (Barcelona), Spain

[2] Univ. Autònoma Barcelona, Cerdanyola del Vallès E-08193 (Barcelona), Spain

[3] Forest Science Centre of Catalonia, Solsona, Catalonia, Spain

[4] Department of Forest Mycology and Plant Pathology, Uppsala Biocenter, Swedish University of Agricultural Sciences, Box 7026, S-750 07 Uppsala, Sweden

[5]Corresponding author: d.aguade@creaf.uab.es

***Keywords*:** die-off, fungi pathogen, global change, hydraulic failure, non-structural carbohydrates

## Abstract

Drought-related tree die-off episodes have been observed in all vegetated continents. Despite much research effort, however, the multiple interactions between carbon starvation, hydraulic failure and biotic agents in driving tree mortality under field conditions are still not well understood.

We analysed the seasonal variability of non-structural carbohydrates (NSC) in four organs (leaves, branches, trunk and roots), the vulnerability to embolism in roots and branches, native embolism (PLC) in branches and the presence of root rot pathogens in defoliated and non-defoliated individuals in a declining Scots pine (*Pinus sylvestris* L.) population in the NE Iberian Peninsula in 2012, which included a particularly dry and warm summer.

No differences were observed between defoliated and non-defoliated pines in hydraulic parameters, except for a higher vulnerability to embolism at pressures below -2 MPa in roots of defoliated pines. No differences were found between defoliation classes in branch PLC.

Total NSC (TNSC, soluble sugars plus starch) values decreased during drought, particularly in leaves. Defoliation reduced TNSC levels across tree organs, especially just before (June) and during (August) drought.

Root rot infection by the fungal pathogen *Onnia* spp. was detected but it did not appear to be associated to tree defoliation. However, *Onnia* infection was associated with reduced leaf specific hydraulic conductivity ($K_L$) and sapwood depth, and thus contributed to hydraulic impairment, especially in defoliated pines. Infection was also associated with virtually depleted root starch reserves during and after drought in defoliated pines. Moreover, defoliated and infected trees tended to show lower Basal Area Increment (BAI).

Overall, our results show the intertwined nature of physiological mechanisms leading to drought-induced mortality and the inherent difficulty of isolating their contribution under field conditions.

## Introduction

Drought-induced tree die-off is emerging as a global phenomenon, affecting a great variety of species and ecosystems in all vegetated continents of the world (Allen et al. 2010). Recent episodes of crown defoliation and tree mortality have been related to an increase of mean annual temperature and a decrease of annual rainfall in southern European forests (Carnicer et al. 2011) and with increasing severe droughts in the southwestern United States (Van Mantgem et al. 2009, Williams et al. 2012). Extreme drought events are expected to become more frequent (IPCC 2013), which could accelerate drought-related tree mortality. These responses can be amplified in many regions by current trends towards increased stand basal area, associated with changes in forest management (Martínez-Vilalta et al. 2012). There are important feedback loops between forest dynamics and climate due to the key role of forests on the global water and carbon cycles (Bonan 2008) and thus widespread forest mortality can have rapid and drastic consequences for ecosystems (Anderegg et al. 2013a). Nonetheless, and despite these potential effects on ecosystem functioning, the mechanisms causing tree die-off are still poorly understood (Sala et al. 2010, McDowell 2011, McDowell et al. 2011).

McDowell et al. (2008) introduced a framework with three main, non-exclusive mechanisms that could cause drought-induced mortality in trees: 1) carbon starvation, 2) hydraulic failure and 3) biotic agents. They also hypothesized that plants with a strict control of water loss through stomatal closure (isohydric species) would be more likely

to die of carbon starvation during a long drought, whereas anisohydric species would more likely experience hydraulic failure during intense droughts, due to more negative xylem water potentials (McDowell et al. 2008). However, the evidence for or against these proposed mortality mechanisms is inconclusive, and recent reports have urged adoption of a more integrated approach focusing on the interrelations between plant hydraulics and the economy and transport of carbon in plants (McDowell and Sevanto 2010, Sala et al. 2010, McDowell 2011, McDowell et al. 2011, Sala et al. 2012).

Xylem vulnerability to embolism has been found to place a definitive limit on the physical tolerance of conifers (Brodribb and Cochard 2009) and angiosperms (Urli et al. 2013) to desiccation. A recent global synthesis has shown that many tree species operate within relatively narrow hydraulic safety margins in all major biomes of the world (Choat et al. 2012). Although structural and physiological acclimation to drought may result in large safety margins from hydraulic failure preceding death (Plaut et al. 2012), high levels of hydraulic dysfunction associated with drought-induced desiccation have been reported (Hoffmann et al. 2011, Nardini et al. 2013). In addition, evidence of hydraulic failure linked to canopy and root mortality has been found in declining trembling aspen (*Populus tremuloides* Michx.), without evidence of depletion of carbohydrate reserves (Anderegg et al. 2012), and in some *Eucalyptus* species (Mitchell et al. 2013).

The dynamics and role of non-structural carbohydrate (NSC) stores during drought are still under debate but some agreement is emerging in that NSC concentrations tend to increase under moderate drought because growth ceases before photosynthesis, whereas they may decline sharply if drought conditions become extreme (McDowell 2011). Recent reports show that the same drought conditions can have contrasting effects on

NSC concentrations even on species of the same genus (*Nothofagus*) (Piper 2011). On the other hand, Galiano et al. (2011) reported extremely low NSC concentrations in the stem of defoliated Scots pine (*Pinus sylvestris* L.) trees and higher probability of drought-induced mortality in pines with lower NSC concentrations. Also, Adams et al. (2013) observed an association between tree mortality and reduced NSC levels in leaves in a drought simulation experiment on piñon pine (*Pinus edulis* Engelm.). In addition, drought-related reductions in stored NSC pools may affect tree organs differentially. For instance, Hartmann et al. (2013a) showed a reduction of NSC in Norway spruce (*Picea abies* (L.) Karst.) roots but not in leaves, which could be attributed to changes in carbon allocation.

Biotic agents and drought can interact to accelerate tree mortality. Drought-stressed trees may be more vulnerable to infection by fungal pathogens (Desprez-Loustau et al. 2006, La Porta et al. 2008) or to insect attacks (Matthias et al. 2007, Gaylord et al. 2013). Although pathogens can directly kill trees through the production of toxic metabolites, they can also induce hydraulic failure, e.g. via occlusion of the xylem, or carbon starvation by altering NSC demand or supply. The interactions between pathogen infection and the physiological mechanisms of drought-induced mortality depend on the trophic interaction (biotrophic, necrotrophic or vascular wilts) established with the tree (Oliva et al. 2014). For instance, blue-stain fungi infection can cause outright hydraulic failure via xylem occlusion (Hubbard et al. 2013) while root rot fungi may lead to a gradual tree decline and eventually to death because of chronic growth reductions and subsequent constraints on water transport (Oliva et al. 2012). In addition, root rot fungi can reduce carbon reserves by fungal consumption of stored carbohydrates or by the induction of carbon-expensive defences, causing tree growth reductions (Cruickshank et al. 2011).

Field studies on mature trees examining all three hypothesized mechanisms of drought-induced mortality are still scarce and rarely explore explicitly the interactions between different mechanisms and their occurrence in different plant organs. Here we compare the hydraulic properties and the dynamics of NSC and embolism as a function of defoliation and infection by fungal pathogens in Scots pine trees growing together in a site affected by drought-induced decline (Martínez-Vilalta and Piñol 2002, Hereş et al. 2012) and close to the dry limit of the distribution of the species. Previous studies have shown that defoliation precedes drought-induced mortality in Scots pine trees from the same or similar sites (Galiano et al. 2011, Poyatos et al. 2013), and that defoliation seems to be an inevitable consequence of drought in the most susceptible individuals rather than an (effective) strategy to cope with it (Poyatos et al. 2013). In this context, we address the following questions: 1) are defoliated Scots pines intrinsically more vulnerable to xylem embolism than non-defoliated ones, providing evidence in favour of hydraulic failure as an important component of the decline process? and, if so, do defoliated trees experience higher levels of native embolism under dry summer conditions? (i.e., are leaf area reductions enough to compensate for their intrinsically higher vulnerability?); 2) do defoliated pines have lower seasonal NSC concentrations in all organs, supporting carbon starvation being involved in the mortality process?; and 3) is infection by fungal pathogens likely to enhance hydraulic dysfunction through increased levels of native embolism, or carbon depletion directly or indirectly lowering NSC levels through increased consumption, reduced sapwood depth or low growth?.

## Materials and methods

*Study site*

The study was conducted in Tillar valley (41° 19' N, 1° 00' E; 990 m a.s.l.) within Poblet Forest Natural Reserve (Prades Mountains, NE Iberian Peninsula). The climate is typically Mediterranean, with a mean annual precipitation of 664 mm (spring and autumn being the rainiest seasons and with a marked summer dry period), and moderately warm temperatures (11.3 °C on average) (Poyatos et al. 2013). The soils are mostly Xerochrepts with fractured schist and clay loam texture, although outcrops of granitic sandy soils are also present (Hereter et al. 1999). Our experimental area is mostly located on a NW-facing hillside with a very shallow and unstable soil due to the high stoniness and steep slopes (35° on average). More detailed information about the study area can be found in Hereter and Sánchez (1999).

The dominant canopy tree species in the study site is Scots pine and the understory consists mainly of the Mediterranean evergreen holm oak (*Quercus ilex* L.). Severe droughts have affected the study site since the 1990's (Martínez-Vilalta and Piñol 2002, Hereş et al. 2012). Scots pine average standing mortality and crown defoliation in the Tillar valley are currently 12% and 52%, respectively. However, in some parts of the forest standing mortality is >20% and cumulative mortality is as high as 50% in the last 20 years (J. Martinez-Vilalta, unpublished data). The Scots pine population studied is more than 150 years old and has remained largely unmanaged for the past 30 years (Hereş et al. 2012). No major insect infestation episode associated with the forest decline in the area has been detected (Mariano Rojo, Catalan Forest Service, pers com.).

A mixed Holm oak – Scots pine stand with a predominantly northern aspect was selected for this study where defoliated and non-defoliated pines were living side by side. A total of 10 defoliated and 10 non-defoliated Scots pine trees were sampled (see Supplementary Table S1). In order to minimize unwanted variation, all trees had a diameter at breast height (DBH) between 25 and 50 cm (average DBH 36.08 ± 1.53 cm;

similar between defoliation classes ($P$>0.05; data not shown)) and the distance between sampled trees was always >5 m (the average minimum distance was 41.99 ± 13.74 m). In this study, defoliation was visually estimated relative to a completely healthy tree in the same population (cf. Galiano et al. 2011). A tree was considered as non-defoliated if the percentage of green needles was >60% (average green leaves of the sampled non-defoliated trees = 77%) and defoliated if the percentage of green needles was <40% (average green leaves of the sampled defoliated trees = 26%). The average height of Scots pines in the population studied was 14.1 ± 0.5 m (Poyatos et al. 2013). All measurements, in combination with a continuous monitoring of the main meteorological variables and soil moisture (cf. Poyatos et al. 2013 for details), were carried out during 2012. Sampling from defoliated trees avoided dead or dying branches (i.e., those with no green leaves), so our sampling can be considered representative only of the living part of the crown.

*Non-structural carbohydrates sampling and analysis*

Trees were sampled in March (late winter), June (late spring), August (mid summer) and October (early autumn). Four organs (leaves, branches, trunk and coarse roots) were sampled from every tree to measure non-structural carbohydrates (NSC). Sun-exposed branches (0.5 – 1 cm of diameter with bark removed) were excised with a pole pruner around noon (12:00 pm – 3:00 pm, local time) to minimize the impact of diurnal variation in NSC concentrations due to photosynthetic activity (Li et al. 2008, Gruber et al. 2012). One-year-old leaves were sampled from these branches. Trunk xylem at breast height and coarse roots at 5-10 cm soil depth were cored to obtain sapwood. Sapwood portion was visually estimated in situ from all the extracted cores. We also used these cores to measure the Basal Area Increment (BAI) corresponding to the three

most recent annual rings (see Supplementary Table S1). All samples were placed immediately in paper bags and stored in a portable cooler containing cold accumulators. One of the defoliated Scots pine trees (tree 1637; see Supplementary Table S1) died during the study period and leaves could not be sampled in August and October; whereas branches could be sampled in August but not in October.

At the end of every sampling day, samples were microwaved for 90 s in order to stop enzymatic activity and oven-dried for 72 h at 65 °C. Samples were then ground to fine powder in the laboratory. Total NSC (TNSC) was defined as including free sugars (glucose and fructose), sucrose and starch, and were analyzed following the procedures described by Hoch et al. (2002) with some minor variations (cf. Galiano et al. 2011). Approximately 12-14 mg of sample powder was extracted with 1.6 ml distilled water at 100 °C for 60 min. After centrifugation, an aliquot of the extract was used for the determination of soluble sugars (glucose, fructose and sucrose), after enzymatic conversion of fructose and sucrose into glucose (invertase from *Saccharomyces cerevisae*) and glucose hexokinase (GHK assay reagent, I4504 and G3293, Sigma-Aldrich). Another aliquot was incubated with an amyloglucosidase from *Aspergillus niger* at 50 °C overnight, to break down all NSC (starch included) to glucose. The concentration of free glucose was determined photometrically in a 96-well microplate reader (Sunrise Basic Tecan, Männedorf, Switzerland) after enzymatic (GHK assay reagent) conversion of glucose to gluconate-6-phospate. Starch was calculated as TNSC minus soluble sugars. All NSC values are expressed as percent dry matter. Throughout the manuscript NSC is used to refer generically to non-structural carbohydrates, while TNSC is used to refer specifically to the total value of NSC (sum of starch and soluble sugars). The relationship between soluble sugars and TNSC will be expressed as SS:TNSC. Finally, we note that due to the current uncertainty in NSC quantification

methodologies (Quentin et al., in review), our results should be considered valid in relative terms (as used here) but not necessarily comparable to the values obtained by other laboratories or using different methods.

*Hydraulic conductivity and vulnerability to xylem embolism*

Hydraulic measurements were taken on the same Scots pine individuals as NSCs, except for one defoliated tree that could not be sampled for hydraulics. Branches and roots were sampled in April and May 2012, respectively, for determining xylem vulnerability curves. We selected branches and roots containing internodal segments 0.4 – 1.1 cm in diameter and ~15 cm in length. Branches were always sampled from the exposed part of the canopy and were 3-5 years old. Root samples were taken at a soil depth of ~20 cm and always from the down slope side of the trunk, in order to control for differences in water availability or soil properties. Sampled branches and roots were always longer than 40 cm and were immediately wrapped in wet cloths and stored inside plastic bags until they were transported to the laboratory on the same day. Once in the laboratory, samples were stored at 4 °C until their vulnerability curves were established within less than three weeks. Right before that, all leaves distal to the measured branch segments were removed and their total area measured with a Li-Cor 3100 Area Meter (Li-Cor Inc., Lincoln, NE, USA).

Vulnerability curves relating the percentage loss of hydraulic conductivity (PLC) as a function of xylem water potential were established using the air injection method (Cochard et al. 1992). Hydraulic conductivity (water flow per unit pressure gradient) was measured using the XYL'EM embolism meter (Bronkhorst, Montigny-Les-Cormeilles, France) using deionised, degassed water (Liqui-Cel Mini-Module degassing membrane) and a pressure head of 4.5 KPa. The bark was removed from all

measurement segments and their ends were cleanly shaved with a sharp razor blade before connecting to the XYL'EM apparatus.

Branch segments were rehydrated with deionized, degassed water prior to determining maximum hydraulic conductivity ($K_{max}$) (Espino and Schenk 2011), leading to stable and consistent $K_{max}$ measurements. Afterwards, all segments (four to six each time) were placed inside a multi-stem pressure chamber with both ends protruding. Then, we raised the pressure inside the chamber to 0.1 MPa (basal value) during 10 min, lowered the pressure, waited 10 min to allow the system to equilibrate, and measured hydraulic conductivity under a low pressure head (4.5 kPa). Stable conductivity readings were usually achieved within 3 min. These measurements were considered to represent the maximum hydraulic conductivity ($K_{max}$) and were used as reference conductivity (PLC = 0) for the purpose of establishing vulnerability curves. We repeated this process, raising the injection pressure stepwise by 0.5 MPa (roots) or 1 MPa (branches), until the actual conductivity of the segment was less than 20% of $K_{max}$, or when we reached 4 MPa. Due to technical limitations, we could not increase the pressure in the chamber over 4 MPa, but only five samples (out of 38) had not reached 80% PLC at this pressure. We fitted vulnerability curves with the following function (Pammenter and Van Der Willigen 1998):

$$PLC = \frac{100}{1+\exp(a(P-P50))} \qquad \text{Equation 1}$$

In this equation, PLC is the percentage loss of hydraulic conductivity, $P$ the applied pressure, $P_{50}$ the pressure (i.e. $-\psi$) causing a 50% PLC, and $a$ is related to the slope of the curve. Parameters were estimated with nonlinear least squares regression. Some vulnerability curves lead to inconsistent results, due to technical problems, and were removed from the analyses. Final sample size was 15 roots (six from defoliated and nine

from non-defoliated trees) and 15 branches (seven from defoliated and eight from non-defoliated trees).

Measurements of $K_{max}$ were used for calculating specific hydraulic conductivity ($K_S$, in $m^2$ $MPa^{-1}$ $s^{-1}$), as the ratio between maximum hydraulic conductivity and mean cross-sectional area of the segment (without bark); and leaf specific conductivity ($K_L$, in $m^2$ $MPa^{-1}$ $s^{-1}$), as the quotient between maximum hydraulic conductivity and distal leaf area. Finally, we calculated the ratio between distal leaf area and cross-sectional area ($A_L$:$A_S$) of each branch segment.

*Monitoring water potentials and native embolism*

We sampled one exposed branch from each of the trees that had been sampled for vulnerability curves (nine defoliated and 10 non-defoliated individuals) monthly from May to August and in October 2012. Midday and predawn leaf water potentials were usually measured *in situ* on nearby defoliated and healthy pines on the same sampling dates. We selected branches at least 40 cm long and containing internodal segments of 4-10 cm length (0.3 – 0.9 cm in diameter). Immediately following excision, branch samples were placed in plastic bags with a small piece of damp paper towel, stored in a bigger bag containing cold accumulators, and transported to the laboratory within 3 h. All branches were sampled before 8 a.m., solar time.

Once in the laboratory, we measured shoot water potential on one terminal shoot per sampled branch using a Scholander-type pressure chamber (PMS Instruments, Corvallis, OR, USA) (except for the initial, May sampling). To measure native embolism, we cut wood segments (4-10 cm in length) underwater from each sampled branch. The bark was removed from the measurement segments and their ends were cleanly shaved with a sharp razor blade before connecting them to the tubing system of the XYL'EM

apparatus to measure native hydraulic conductivity ($K_i$) under a pressure head of ca. 4.5 kPa. Measurement samples were rehydrated overnight and their maximum hydraulic conductivity ($K_{max}$) was measured with the XYL'EM apparatus as described above. The percentage loss of conductivity due to embolism (PLC) was computed as:

$$PLC = 100\ (\ 1 - \frac{Ki}{Kmax}\ ) \qquad \text{Equation 2}$$

*Root rot pathogens*

We focused on root and butt rot pathogens as possible contributors to the decline process observed in the forest studied. From each tree, we extracted two cores with an increment borer, one at stump height and the other in one of the large roots. Decay presence was noted and cores were kept in sterile conditions. Within 48 hours, they were placed onto Hagem medium amended with benomyl (10 mg/l) and cloramphenicol (200 mg/l). Plates were checked weekly during the following 3 months, and any mycelia growth was sub-cultured. Identification of fungal isolates was first attempted by sequencing the ITS region. Some of our isolates showed an equally low similarity (95%) to other isolates classified as either *Onnia tomentosa* (Fr.) P. Karst. or *O. circinata* (Fr.) P. Karst. in reference databases such as Genbank or UNITE. We identified our cultures as *Onnia* spp., as morphological characters in culture and comparison with reference cultures from CBS-KNAW Fungal Biodiversity Centre (CBS 246.30 *Onnia circinata*, CBS 278.55 *Onnia tomentosa*) did not yield a conclusive identification.

We found signs of fungi infection after the cultivation of the extracted cores in seven pines; three of them were non-defoliated and the other four were defoliated (see Supplementary Table S1). One defoliated and one non-defoliated tree were infected by

a heart rot fungi (*Porodaedalea pini* (Brot.) Murrill). These fungi mainly cause heartwood decay with no major known physiological effects (Garbelotto 2004), so we considered these two trees as 'non-infected' in our analyses. The other trees (two non-defoliated and three defoliated) were infected by *Onnia* sp., which causes root rot and physiological impairment, and we considered those trees as 'infected' in subsequent analyses.

*Data analysis*

We used different types of linear models to test the effects of defoliation and fungal infection on the measured response variables (RV). In each case we included the main covariates (measured organ and sampling month, as appropriate) and the most biologically plausible interactions. Please note that model complexity, in terms of the number of interactions that could be included, is subject to sample size limitations. Preliminary analyses showed that DBH effects were never significant in the models and therefore were not included in the final models reported here. General linear models were fitted to study the effects of defoliation class (two levels: defoliated or non-defoliated) and infection occurrence (two levels: infected or non-infected) on $K_L$, $A_L$:$A_S$, BAI and root and trunk sapwood depths. Separate linear models were fitted for each of the five response variables (see Supplementary data, equation 1). Linear mixed models were used to analyze vulnerability curve parameters ($a$ and $P_{50}$) and $K_S$ as a function of defoliation class, organ (branch or root) and infection occurrence. Tree identity was included in the models as a random factor (see Supplementary data, equation 2). Similar mixed models were used to analyze shoot water potential, PLC, TNSC and SS:TNSC as a function of defoliation class, sampling date, organ (only for TNSC and SS:TNSC), and infection occurrence, including again tree identity as a random factor (see

Supplementary data, equation 3 and equation 4). Finally, starch concentration in roots was also analysed using similar models (without the organ effect) to study in detail the impact of root rot pathogens on this NSC fraction and how it developed over time (and hence in this model we included the interaction between defoliation class, infection occurrence and sampling date) (see Supplementary data, equation 5).

Variables $K_S$, $K_L$, $A_L$:$A_S$, TNSC and root and trunk sapwood depth were log-tranformed, and starch concentration in roots was square root-transformed, to achieve normality prior to all analyses. All analyses were carried out with R Statistical Software version 3.1.0 (R Core Team 2014) using the lm and lme functions.

## Results

*Meteorological conditions*

The summer of 2012 was particularly dry and warm compared to the climatic average for the period 1951-2010: average air temperature (June-August) was 20.56 °C and total precipitation only 56 mm (Fig. 1), compared to climatic values (1951-2010) of 19.30 °C and 135.23 mm, respectively. High values of daytime-averaged temperatures and VPD's (vapour pressure deficit) occurred in mid-August, followed by very low SWC (soil water content) values (~0.08 $m^3$ $m^{-3}$) at the beginning of September, compared to a spring maximum soil moisture of 0.33 $m^3$ $m^{-3}$ (Fig. 1).

*Non-structural carbohydrates*

Concentrations of total non-structural carbohydrates varied among tree organs, in the following order: TNSC (leaves)>TNSC (branches)>TNSC (roots)>TNSC (trunk) (Fig. 2; Table 1). In general, non-defoliated Scots pine trees showed higher concentrations of TNSC throughout the study period and across all organs (Fig. 2). TNSC values

increased from March to June (except for leaves of defoliated pines) to reach a seasonal peak and then declined in August. Seasonal variation in TNSC was greater in leaves, especially for non-defoliated pines, which showed a more than fourfold decline in TNSC between the June peak and the minimum value in August. Post-drought October TNSC only slightly increased in trunks and leaves (Fig. 2). Infection by fungal pathogens was not associated with significant differences in TNSC levels in any organ or month (Table 1).

The ratio of soluble sugars to TNSC (SS:TNSC) differed among tree organs but showed consistent seasonal dynamics across organs (Fig. 2, Table 1). The value of SS:TNSC declined slightly from March to June, it increased in August, especially in leaves, and then declined in October. In August, SS:TNSC values were above 0.8 for all organs and defoliation classes, indicating that most of the TNSC were in the form of soluble sugars (Fig. 2). Starch levels at peak drought were virtually depleted in leaves (i.e. SS:TNSC was nearly 1). Moreover, there were significant differences in SS:TNSC between defoliation classes in some organs and months, whereby defoliated pines tended to show higher SS:TNSC values before the onset of drought but similar or lower values in August (Fig. 2, Table 1). No differences in SS:TNSC were observed associated to fungi infection (Table 1).

Throughout the season, root starch tended to be lower in defoliated pines compared to non-defoliated ones (Fig. 3). Root rot infection was associated with higher root starch levels in non-defoliated pines, but this effect was not observed in defoliated pines (Fig. 3, Table 1). The triple interaction between month, defoliation and infection was statistically significant (Table 1). Interestingly, our results show that root starch concentration in October was virtually depleted in infected, defoliated pines, and it was much lower than in non-infected ones (Fig. 3).

*Vulnerability curves and hydraulic properties*

Roots were more vulnerable to embolism than branches, reaching 50% PLC slightly below -2 MPa, compared to a value close to -3 MPa for branches (Fig. 4). This effect was statistically significant (overall *P*-value for Organ = 0.0062 in a least significant means multiple comparison), although the difference was not significant for all the combinations of defoliation and infections classes (cf. Table 2). The vulnerability to embolism of branches was similar between defoliation classes (Fig. 4b, Table 2). In roots, there was no difference between defoliation classes in $P_{50}$, but the slope of the vulnerability curve was steeper in defoliated trees (Table 2). This result implies that the roots of non-defoliated pines would begin to lose conductivity at higher (i.e., closer to zero) water potentials than those of defoliated individuals, but the latter would lose conductivity faster than non-defoliated pines as water potentials declines (Fig. 4a). Infection did not affect vulnerability to xylem embolism (Table 2).

No differences in specific hydraulic conductivity ($K_s$) were found between roots and branches (Table 2), possibly due, at least in part, to the large variability in $K_s$ observed for roots. Likewise, there were no significant differences in either $K_S$, $K_L$, or $A_L$:$A_S$ between defoliated and non-defoliated pines (Table 2). However, we found lower branch $K_L$ in infected trees (Table 2).

*Water potentials and native embolism*

Shoot water potentials measured in the morning, at the time of sampling for PLC measurements, increased from June to July (Fig. 5b, Table 3), consistent with the rainfall events occurring in late June (Fig. 1). Afterwards, water potentials declined sharply down to values around -2 MPa in August, coinciding with the driest part of the

study period. These water potentials were usually between the corresponding predawn and midday shoot water potentials measured in simultaneous sampling campaigns in nearby Scots pine individuals (Fig. 5c). We did not find any significant effect of defoliation or infection on water potential (Table 3).

Native PLC varied significantly among sampling dates, following the variation in shoot water potentials. PLC was particularly low in July, with values around 20%, and it was highest in August, with average values around 65% (Fig. 5a, Table 3). In August, six branches (four from non-defoliated, and two from defoliated pines) showed PLC values above 85%. Native embolism was not significantly different between defoliation or infection classes (Table 3), except for October when non-defoliated pines showed higher PLC (Fig. 5b) ($P = 0.048$).

*Basal area increment and sapwood depth*

We found a marginally significant reduction of BAI associated with defoliation ($P = 0.064$) and this effect tended to be larger in infected trees as shown by the marginally significant ($P = 0.083$) interaction between defoliation and infection (Fig. 6a).

Trunk sapwood depth showed patterns similar to those for BAI, but with significantly lower values for defoliated and infected individuals (Fig. 6b). Finally, infected trees showed a significantly lower root sapwood depth compared to non-infected trees ($P = 0.039$), regardless of defoliation class; whereas defoliation had no significant effect on root sapwood depth (Fig. 6c) ($P = 0.89$).

## Discussion

Our results show that both high levels of embolism and low carbohydrate reserves occurred in the studied trees during a particularly dry summer. In addition, we show that

defoliation was more associated with reduced carbohydrate reserves than with greater hydraulic impairment at the branch level. We also report that drought-induced defoliation and infection by a root rot fungus occur independently, but they both interact to determine the mode of physiological failure in Scots pine at the dry edge of its distribution. We note, however, that some of these results (particularly those regarding pathogen infection) should be interpreted with caution due to the low sample size.

*Defoliation is associated with lower carbon availability, but not with higher hydraulic impairment at the branch level*

We found no consistent differences between defoliated and non-defoliated pines in terms of their vulnerability to embolism according to $P_{50}$ values. This is consistent with previous studies comparing Scots pine populations suffering different levels of drought-induced decline in the same area (Martinez-Vilalta et al. 2002). Although we found steeper vulnerability curves for roots of defoliated pines, which would yield comparatively higher root PLC at water potentials lower than *ca.* -2 MPa (Fig. 4a), these conditions only occur during exceptional droughts (Poyatos et al. 2013). In addition, branch-level leaf $K_S$ and $A_L$:$A_S$ were similar for defoliated and non-defoliated pines, in contrast with different values observed across Scots pine populations within the same study area (Martínez-Vilalta and Piñol 2002) and with the lower $A_L$:$A_S$ reported at the tree level for defoliated pines (Poyatos et al. 2013). It should be emphasized, however, that our sampling design is representative at the branch level, but not necessarily at the whole crown level, as we were forced to sample living (as opposed to random) branches in heavily defoliated crowns.

It is also interesting to note that our results show a slightly higher branch vulnerability to embolism compared to the $P_{50}$ of ~-3.2 MPa reported previously for the same

population (Martínez-Vilalta and Piñol 2002). This result may be related to some sort of filtering at the population level (i.e., preferential mortality of pines with higher resistance to embolism) or a by-product of the large variability in $P_{50}$ observed across branches. But it is also possible that vulnerability to embolism may be increasing over time as a result of repeated droughts (i.e. cavitation fatigue; Hacke et al. (2001)), as it has been reported in the case of aspen die-off (Anderegg et al. 2013b).

The decline in PLC observed after a rainy period in July (Fig. 5a) suggests some partial embolism reversal (e.g. McCulloh et al. 2011), but we cannot rule out the possibility that sampling artefacts may be causing an overestimation of this PLC recovery (e.g. Sperry 2013). Although our results imply that defoliation may be relatively effective in avoiding further increases in branch PLC, maximum PLC values were still within a range (*ca.* 50-90%) associated with canopy dieback in several angiosperms (Hoffmann et al. 2011, Anderegg et al. 2012, Anderegg et al. 2013b, Nardini et al. 2013) and gymnosperms (Klein et al. 2012, Plaut et al. 2012). Overall, these results also suggest that the steeper declines in whole-plant hydraulic conductance observed for defoliated pines during drought (Poyatos et al. 2013) may occur primarily belowground, as observed in other pine species prior to death (Plaut et al. 2013).

Defoliated pines showed consistently lower TNSC values than non-defoliated pines for most combinations of organ and season, as already observed in early autumn measurements of stem TNSC in other declining Scots pine populations (Galiano et al. 2011), including the study site (Poyatos et al. 2013). Interestingly, we did not observe increased TNSC in leaves of defoliated pines, despite their higher assimilation rates (Mencuccini et al., unpublished data). TNSC decreased in all organs during drought,

and most dramatically in leaves, tracking the seasonality of gas exchange (Poyatos et al. 2013).

The observed seasonal variation of the fraction of soluble sugars (SS:TNSC) (Fig. 2) is consistent with starch concentration building up prior to bud-break and then decreasing during the summer period (Hoch and Körner 2003, Gruber et al. 2012). During August, the greater mobilization of starch to soluble sugars could be attributed to several causes, including osmoregulation (Sala et al. 2012), the de novo synthesis of carbon-rich compounds into defence against root rot pathogens (Oliva et al. 2012), the energy-dependent process of embolism repair (Brodersen and McElrone 2013) and the growth of new tissue. The two latter processes are consistent with the reduction of native embolism after August, reaching pre-drought values in October (Fig. 5a).

Despite the combination of drought and defoliation, our results did not show a complete depletion of TNSC in any of the organs studied (Fig. 2), even in the tree that died during the monitoring period (data not shown). Values of trunk TNSC as low as 0.1% were measured in Scots pine one year prior to death in a nearby population (Galiano et al. 2011) while our trunk TNSC values were always >0.4%. Experimental studies on conifer saplings (Hartmann et al. 2013b), including pine species (Mitchell et al. 2013), have found evidence for drastic reductions in TNSC (especially starch) in stems and/or roots at mortality, without actually showing completely depleted carbohydrate storage. Phloem impairment may preclude the translocation of NSC and its availability for the maintenance of xylem transport or for the production of defence compounds (Sala et al. 2010, Sevanto et al. 2013, Hartmann et al. 2013a). A recent modelling analysis in the same study system predicts slow, but not disrupted, phloem transport under extreme drought (Mencuccini et al., unpublished data).

*Root rot pathogens exacerbate hydraulic and carbon-related constraints at the tree level*

We did not find a clear BAI reduction in *Onnia*-infected trees (Fig. 6a), contrary to other studies reporting growth reductions caused by root rot pathogens from the *Armillaria* (Cruickshank et al. 2011) and *Heterobasidion* genus (Oliva et al. 2012). Although the interaction between infection and defoliation was only marginally significant, the trend towards lower BAI in trees that were both defoliated and infected would be consistent with the reduced sapwood depth observed in these trees (Fig. 6b). Hence, post-drought recovery of xylem specific hydraulic conductivity would be severely constrained in the long-term. Lower sapwood depth in the roots of infected trees (Fig. 6c), could be the ultimate consequence of the decay progress, due to the reduction of tree growth caused by the formation of a reaction zone (Oliva et al. 2012). Infection-driven reductions in sapwood depth in roots (and in the trunk of infected, defoliated trees) may also result in lower tissue capacitance and a decreased ability to buffer short-term variations in water potential under drought (McCulloh et al. 2014).

Even though *Onnia* infection did not affect the vulnerability to embolism, it was associated with reduced $K_L$, particularly in defoliated pines (Table 2). Hence, infection by a root rot pathogen likely exacerbated hydraulic constraints through effects on growth and sapwood depth but also more directly through its impact on hydraulic conductivity.

Our results show a complex picture of the root rot infection effects on NSC pools. We did not find any evidence for consistent reductions in TNSC across tree organs associated with *Onnia* infection. However, for non-defoliated pines, infection appeared to drive starch accumulation in roots, rather than depletion, possibly as a response to increased sink strength in the roots associated to higher C demand (de novo synthesis of

defence compounds; Oliva et al. 2014). Presumably, defoliated pines were so severely carbon-limited that this starch sink in the roots could not be maintained, and they ended the year with extremely low levels of starch in roots (Fig. 3). These findings are in line with a recently proposed framework, which postulates that the net effect of the infection by a necrotrophic pathogen, such as *Onnia*, is strongly dependent on tree C availability and the timing of drought events (Oliva et al. 2014).

*A complex pathway to mortality*

In this final section we synthesize our current understanding on the process of drought-induced mortality in the study area, from the perspective of the comparison of coexisting defoliated and healthy individuals, using the information gathered here and in other studies conducted at the same site (Fig. 7). Drought-induced defoliation is associated with drier microenvironments (Vilà-Cabrera et al. 2013) and with steeper reductions of whole-plant hydraulic conductance during seasonal drought (Poyatos et al. 2013). Hydraulic constraints may be related to higher vulnerability to embolism in roots (steeper vulnerability curves) and can be magnified by cavitation fatigue following repeated droughts. Defoliation and prolonged periods of near complete stomatal closure both contribute to reduce NSC in defoliated trees (Poyatos et al. 2013). Defoliated trees appear to enter a death spiral in which reduced C assimilation constrains radial growth (Hereş et al. 2012) and crown development (Poyatos et al. 2013). Root rot fungi may further damage hydraulic function through direct effects on sapwood depth and cumulative growth reductions. Moreover, the demand for C-rich compounds for osmoregulation, hydraulic repair and defence against root rot infection may contribute to the depletion of C reserves in defoliated pines, possibly increasing the minimum C threshold for tree survival and hence accelerating tree mortality (Oliva et al. 2014). It

remains to be established whether the framework outlined in Fig. 7, which has been developed for only one species in a given region, can be applied to other species and study systems. Overall, our study reflects the intertwined nature of physiological mechanisms leading to drought-induced mortality (McDowell et al. 2011) and the inherent difficulty of isolating their contribution under field conditions.

## Supplementary data

Supplementary data for this article are available at Tree Physiology Online.

## Acknowledgements

We would like to thank L. Galiano and T. Rosas for assistance in field sampling and carbohydrates analysis. We also thank all the staff from the Poblet Forest Natural Reserve for allowing us to carry out research at the "Barranc del Tillar" and for their logistic support in the field. The comments by Rick Meinzer and two anonymous reviewers greatly improved the manuscript.

## Conflict of interest

None declared.

## Funding

Competitive grants CGL2010-16373 and CSD2008-0004, a Juan de la Cierva postdoctoral fellowship awarded to R.P., and a FPU doctoral fellowship through the Spanish Ministry of Education, Culture and Sport awarded to D.A.

## References

Adams HD, Germino MJ, Breshears DD, Barron-Gafford GA, Guardiola-Claramonte M, Zou CB, Huxman TE (2013) Nonstructural leaf carbohydrate dynamics of *Pinus edulis* during drought-induced tree mortality reveal role for carbon metabolism in mortality mechanism. New Phytol 197:1142-1151.

Allen CD, Macalady AK, Chenchouni H, Bachelet D, McDowell N, Vennetier M, Kitzberger T, Rigling A, Breshears DD, Hogg EH (2010) A global overview of drought and heat-induced tree mortality reveals emerging climate change risks for forests. For Ecol Manag 259:660-684.

Anderegg WRL, Berry JA, Smith DD, Sperry JS, Anderegg LDL, Field CB (2012) The roles of hydraulic and carbon stress in a widespread climate-induced forest die-off. Proc. Nat. Acad. Sci 109:233-237.

Anderegg WRL, Kane JM, Anderegg LDL (2013a) Consequences of widespread tree mortality triggered by drought and temperature stress. Nature Clim Change 3:30-36.

Anderegg WRL, Plavcová L, Anderegg LDL, Hacke UG, Berry JA, Field CB (2013b) Drought's legacy: multiyear hydraulic deterioration underlies widespread aspen forest die-off and portends increased future risk. Glob Change Biol 19:1188-1196.

Bonan, GB (2008) Forests and climate change: forcings, feedbacks, and the climate benefits of forests. Science 320:1444-1449.

Brodersen CR, McElrone, AJ (2013) Maintenance of xylem network transport capacity: a review of embolism repair in vascular plants. Front Plant Sci 4.

Brodribb TJ, Cochard H (2009) Hydraulic failure defines the recovery and point of death in water-stressed conifers. Plant Physiol 149:575-584.

Carnicer J, Coll M, Ninyerola M, Pons X, Sánchez G, Peñuelas J (2011) Widespread crown condition decline, food web disruption, and amplified tree mortality with increased climate change-type drought. Proc. Nat. Acad. Sci 108:1474-1478.

Choat B, Jansen S, Brodribb TJ, Cochard H, Delzon S, Bhaskar R, Bucci SJ, Feild TS, Gleason SM, Hacke UG, Jacobsen AL, Lens F, Maherali H, Martínez-Vilalta J, Mayr S, Mencuccini M, Mitchell PJ, Nardini A, Pittermann J, Pratt RB, Sperry JS, Westoby M, Wright IJ, Zanne AE (2012) Global convergence in the vulnerability of forests to drought. Nature 491:752-755.

Cochard H, Cruiziat P, Tyree MT (1992) Use of Positive Pressures to Establish Vulnerability Curves. Further Support for the Air-Seeding Hypothesis and Implications for Pressure-Volume Analysis. Plant Physiol 100:205-209.

Cruickshank MG, Morrison DJ, Lalumière A (2011) Site, plot, and individual tree yield reduction of interior Douglas-fir associated with non-lethal infection by Armillaria root disease in southern British Columbia. For Ecol Manag 261:297-307.

Desprez-Loustau ML, Marçais B, Nageleisen LM, Piou D, Vannini A (2006) Interactive effects of drought and pathogens in forest trees. Ann Sci For 63:597-612.

Espino S, Schenk HJ (2011) Mind the bubbles: achieving stable measurements of maximum hydraulic conductivity through woody plant samples. J Exp Bot 62:1119-1132.

Galiano L, Martínez-Vilalta J, Lloret F (2011) Carbon reserves and canopy defoliation determine the recovery of Scots pine 4 yr after a drought episode. New Phytol 190:750-759.

Garbelotto M (2004) Root and butt rot diseases. In: Burley J, Evan J, Youngquist JA (eds) The encyclopedia of forest sciences. Elsevier, Oxford, pp 750-758.

Gaylord ML, Kolb TE, Pockman WT, Plaut JA, Yepez EA, Macalady AK, Pangle RE, McDowell NG (2013) Drought predisposes piñon-juniper woodlands to insect attacks and mortality. New Phytol 198:567-578.

Gruber A, Pirkebner D, Florian C, Oberhuber W (2012) No evidence for depletion of carbohydrate pools in Scots pine (*Pinus sylvestris* L.) under drought stress. Plant Biol 14:142-148.

Hacke UG, Stiller V, Sperry JS, Pittermann J, McCulloh KA (2001) Cavitation fatigue. Embolism and refilling cycles can weaken the cavitation resistance of xylem. Plant Physiol 125:779-786.

Hartmann H, Ziegler W, Kolle O, Trumbore S (2013a) Thirst beats hunger-declining hydration during drought prevents carbon starvation in Norway spruce saplings. New Phytol 200:340-349.

Hartmann H, Ziegler W, Trumbore S (2013b) Lethal drought leads to reduction in nonstructural carbohydrates in Norway spruce tree roots but not in the canopy. Funct Ecol 27:413-427.

Hereş A-M, Martínez-Vilalta J, López BC (2012) Growth patterns in relation to drought-induced mortality at two Scots pine (*Pinus sylvestris* L.) sites in NE Iberian Peninsula. Trees-Struct Funct 26:621-630.

Hereş A-M, Voltas J, López BC, Martínez-Vilalta J (2013) Drought-induced mortality selectively affects Scots pine trees that show limited intrinsic water-use efficiency responsiveness to raising atmospheric $CO_2$. Funct Plant Biol 41:244-256.

Hereter A, Sánchez JR (1999) Experimental areas of Prades and Montseny. In: Rodà F, Retana J, Gracia CA, Bellot J (eds) Ecology of Mediterranean evergreen oak forests. Springer, Berlin, Heidelberg, pp 15–27.

Hoch G, Körner C (2003) The carbon charging of pines at the climatic treeline: a global comparison. Oecologia 135:10-21.

Hoch G, Popp M, Körner C (2002) Altitudinal increase of mobile carbon pools in *Pinus cembra* suggests sink limitation of growth at the Swiss treeline. Oikos 98:361-374.

Hoffmann WA, Marchin RM, Abit P, Lau OL (2011) Hydraulic failure and tree dieback are associated with high wood density in a temperate forest under extreme drought. Glob Change Biol 17:2731-2742.

Hubbard RM, Rhoades CC, Elder K, Negron J (2013) Changes in transpiration and foliage growth in lodgepole pine trees following mountain pine beetle attack and mechanical girdling. For Ecol Manag 289:312-317.

IPCC. 2013 Climate Change 2013: The Physical Science Basis. Contribution of Working Group I to the Fifth Assessment Report of the Intergovernmental Panel on Climate Change (IPCC). Cambridge University Press, Cambridge, UK and New York, NY, USA, 1535 pp.

Klein T, Di Matteo G, Rotenberg E, Cohen S, Yakir D (2012) Differential ecophysiological response of a major Mediterranean pine species across a climatic gradient. Tree Physiol 33(1):26-36.

La Porta N, Capretti P, Thomsen IM, Kasanen R, Hietala AM, Von Weissenberg K (2008) Forest pathogens with higher damage potential due to climate change in Europe. Can J Plant Pathol 30:177-195.

Li MH, Xiao WF, Wang SG, Cheng GW, Cherubini P, Cai XH, Liu XL, Wang XD, Zhu WZ (2008) Mobile carbohydrates in Himalayan treeline trees I. Evidence for carbon gain limitation but not for growth limitation. Tree Physiol 28:1287-1296.

Martínez-Vilalta J, Lloret F, Breshears DD (2012) Drought-induced forest decline: causes, scope and implications. Biol Letters 8:689-691.

Martínez-Vilalta J, Piñol J (2002) Drought-induced mortality and hydraulic architecture in pine populations of the NE Iberian Peninsula. For Ecol Manag 161:247-256.

Matthias D, Beat W, Christof B, Matthias B, Mathias C, Beat F, Urs G, Andreas R (2007) Linking increasing drought stress to Scots pine mortality and bark beetle infestations. Scientific World Journal 7:231-239.

McCulloh KA, Johnson DM, Meinzer FC, Lachenbruch B (2011) An annual pattern of native embolism in upper branches of four tall conifer species. Am J Bot 98:1007-1015.

McCulloh KA, Johnson DM, Meinzer FC, Woodruff DR (2014) The dynamic pipeline: hydraulic capacitance and xylem hydraulic safety in four tall conifer species. Plant Cell Environ 37:1171-1183.

McDowell N, Pockman WT, Allen CD, Breshears DD, Cobb N, Kolb T, Plaut J, Sperry J, West A, Williams DG, Yepez EA (2008) Mechanisms of plant survival and mortality during drought: why do some plants survive while others succumb to drought? New Phytol 178:719-739.

McDowell NG (2011) Mechanisms linking drought, hydraulics, carbon metabolism, and vegetation mortality. Plant Physiol 155:1051-1059.

McDowell NG, Beerling DJ, Breshears DD, Fisher RA, Raffa KF, Stitt M (2011) The interdependence of mechanisms underlying climate-driven vegetation mortality. Trends Ecol Evol 26:523-532.

McDowell NG, Sevanto S (2010) The mechanisms of carbon starvation: how, when, or does it even occur at all? New Phytol 186:264-266.

Mitchell PJ, O'Grady AP, Tissue DT, White DA, Ottenschlaeger ML, Pinkard EA (2013) Drought response strategies define the relative contributions of hydraulic dysfunction and carbohydrate depletion during tree mortality. New Phytol 197:862-872.

Nardini A, Battistuzzo M, Savi T (2013) Shoot desiccation and hydraulic failure in temperate woody angiosperms during an extreme summer drought. New Phytol 200:322-329.

Oliva J, Camarero J, Stenlid J (2012) Understanding the role of sapwood loss and reaction zone formation on radial growth of Norway spruce (*Picea abies*) trees decayed by *Heterobasidion annosum* s.l. For Ecol Manag 274:201-209.

Oliva J, Stenlid J, Martínez-Vilalta J (2014) The effect of fungal pathogens on the water and carbon economy of trees: implications for drought-induced mortality. New Phytol DOI: 10.1111/nph.12857.

Pammenter NW, Van Der Willigen C (1998) A mathematical and statistical analysis of the curves illustrating vulnerability of xylem to cavitation. Tree Physiol 18:589-593.

Piper FI (2011) Drought induces opposite changes in the concentration of non-structural carbohydrates of two evergreen *Nothofagus* species of differential drought resistance. Ann Sci For 68:415-424.

Plaut JA, Wadsworth WD, Pangle R, Yepez EA, McDowell NG, Pockman WT (2013) Reduced transpiration response to precipitation pulses precedes mortality in a piñon-juniper woodland subject to prolonged drought. New Phytol 200:375-387.

Plaut JA, Yepez EA, Hill J, Pangle R, Sperry JS, Pockman WT, McDowell NG (2012) Hydraulic limits preceding mortality in a piñon-juniper woodland under experimental drought. Plant Cell Environ 35:1601-1617.

Poyatos R, Aguadé D, Galiano L, Mencuccini M, Martínez-Vilalta J (2013) Drought-induced defoliation and long periods of near-zero gas exchange play a key role in accentuating metabolic decline of Scots pine. New Phytol 200:388-401.

R Core Team (2014). R: A language and environment for statistical computing. R Foundation for Statistical Computing, Vienna, Austria. URL http://R-project.otg/.

Sala A, Piper F, Hoch G (2010) Physiological mechanisms of drought induced tree mortality are far from being resolved. New Phytol 186:274-281.

Sala A, Woodruff DR, Meinzer FC (2012) Carbon dynamics in trees: feast or famine? Tree Physiol 32:764-775.

Sevanto S, McDowell NG, Dickman LT, Pangle R, Pockman WT (2013) How do trees die? A test of the hydraulic failure and carbon starvation hypotheses. Plant Cell Environ 37:153-161.

Sperry J (2013) Cutting-edge research or cutting-edge artefact? An overdue control experiment complicates the xylem refilling story. Plant Cell Environ 36:1916-1918.

Urli M, Porté AJ, Cochard H, Guengant Y, Burlett R, Delzon S (2013) Xylem embolism threshold for catastrophic hydraulic failure in angiosperm trees. Tree Physiol 33:672-683.

Van Mantgem PJ, Stephenson NL, Byrne JC, Daniels LD, Franklin JF, Fule PZ, Harmon ME, Larson AJ, Smith JM, Taylor AH (2009) Widespread increase of tree mortality rates in the western United States. Science 323:521-524.

Vilà-Cabrera A, Martínez-Vilalta J, Galiano L, Retana J (2013) Patterns of forest decline and regeneration across Scots pine populations. Ecosystems 16:323-335.

Williams AP, Allen CD, Macalady AK, Griffin D, Woodhouse CA, Meko DM, Swetnam TW, Rauscher SA, Seager R, Grissino-Mayer HD (2012) Temperature as a potent driver of regional forest drought stress and tree mortality. Nature Clim Change 3:292-297.

## Figure legends

Figure 1. Seasonal course of daily precipitation, soil water content (SWC), vapor pressure deficit (VPD) and temperature during the study period. Error bars indicate ± 1 SE. Arrows in the upper panel indicate sampling days (carbohydrates sampling: solid arrow; carbohydrates + embolism sampling: dotted arrow; embolism sampling: dashed arrow).

Figure 2. Seasonal variation of total non-structural carbohydrates (TNSC) and the ratio between soluble sugars and total non-structural carbohydrates (SS:TNSC) in the four studied organs. Error bars indicate ± 1 SE. The asterisks indicate significant differences between defoliation classes within a given sampling month (• $0.05<P<0.1$; * $0.01<P<0.05$; ** $0.001<P< 0.01$; *** $P<0.001$).

Figure 3. Seasonal changes in root starch concentration as a function of infection and defoliation classes. Error bars indicate ± 1 SE.

Figure 4. Vulnerability curves for roots (a) and branches (b) of defoliated and non-defoliated Scots pine trees, showing percentage loss of hydraulic conductivity (PLC) as a function of applied pressure. Equation 1 was used to fit the curves. Error bars indicate ± 1 SE.

Figure 5. Seasonal variation of (a) native embolism expressed as percentage loss of hydraulic conductivity (PLC) and (b) corresponding water potential, measured in the same branches, of defoliated and non-defoliated Scots pine trees. Panel (c) shows predawn and midday water potentials from nearby Scots pine trees from the same population measured on the same dates, where solid lines and symbols indicate defoliated trees and dashed lines and open symbols designate non-defoliated individuals.

Error bars indicate ± 1 SE. Different letters indicate significant differences ($P$<0.05) between sampling dates.

Figure 6. Basal area increment (BAI) (a), trunk sapwood depth (b), and root sapwood depth (c) as a function of infection and defoliation classes. Different uppercase letters indicate significant differences ($P$<0.05) between infestation occurrence, and different lowercase letters indicate significant differences between defoliation classes within a given infection class. Note that the interaction between defoliation and infection in the BAI model was marginally significant (0.05<$P$<0.1). Error bars ± 1 SE.

Figure 7. Schematic diagram of the processes associated with drought-induced mortality in Scots pine at our study site in Prades. Different numbers depict studies where the relationship has been reported: 1) Vilà-Cabrera et al. 2013, Poyatos et al. 2013, 2) Poyatos et al. 2013, 3) Poyatos et al. 2013, 4) Hereş et al. 2013, 5) Hereş et al. 2012 and 6) Galiano et al. 2011. Only Galiano et al. 2011 refers to a study conducted in a nearby population. Arrows indicate relationship between mechanisms. Dashed lines depict the relationships examined in this study. Question marks identify consequences for which the evidence is still weak. Letters inside "Tree NSC storage" compartment indicate different levels of NSC: A) high levels (tree survives), B) medium levels (tree survives), and C) low levels (tree dies).

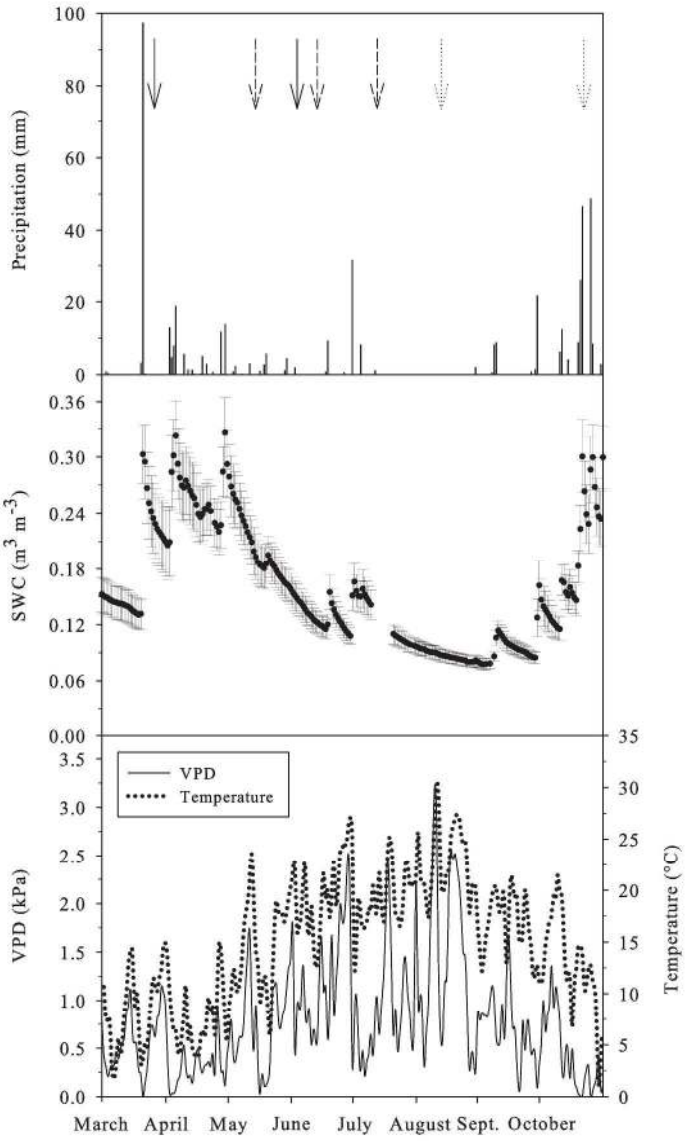


233x406mm (300 x 300 DPI)

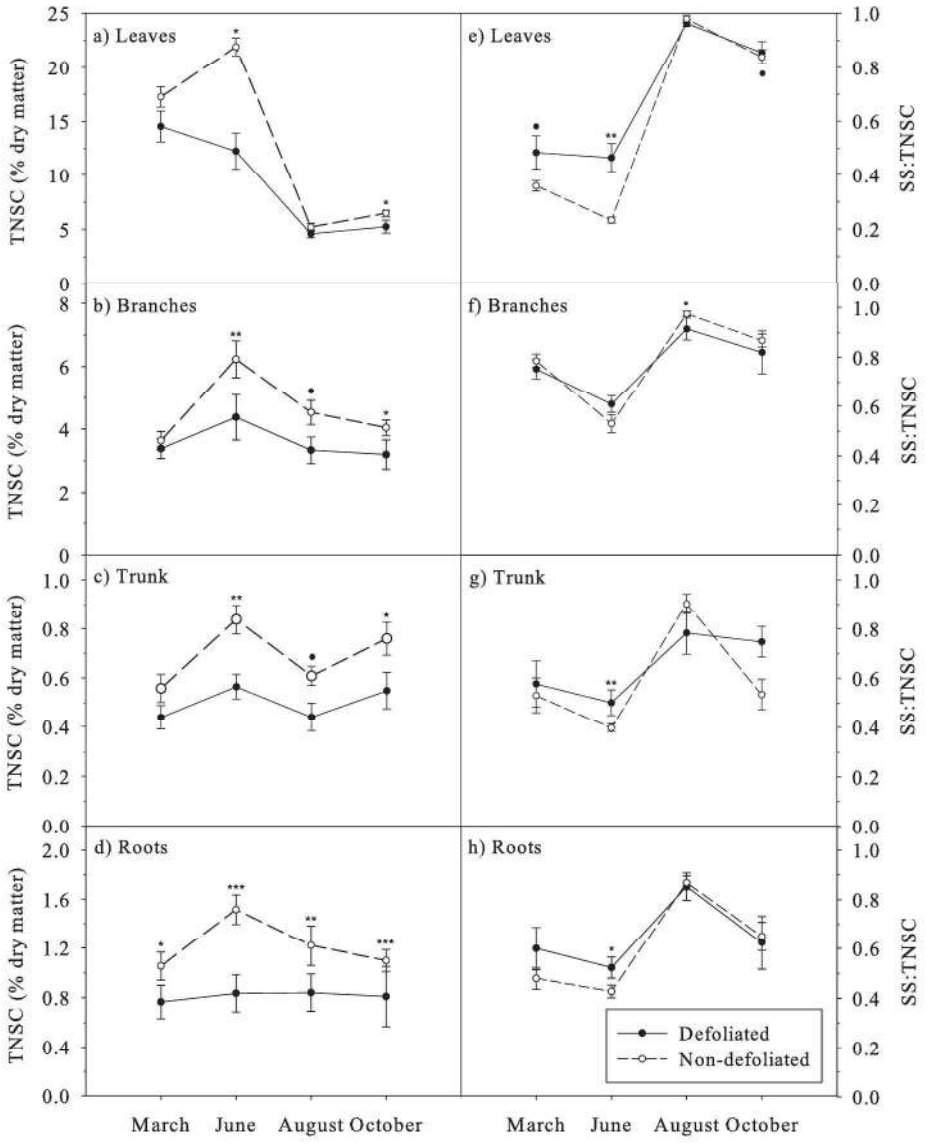


233x303mm (300 x 300 DPI)

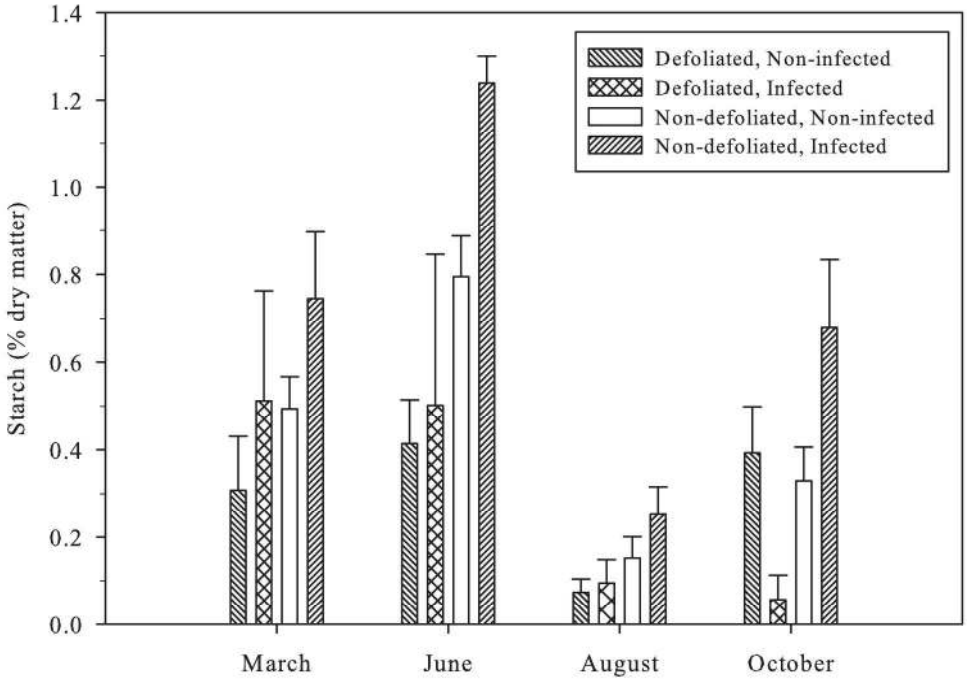


233x176mm (300 x 300 DPI)

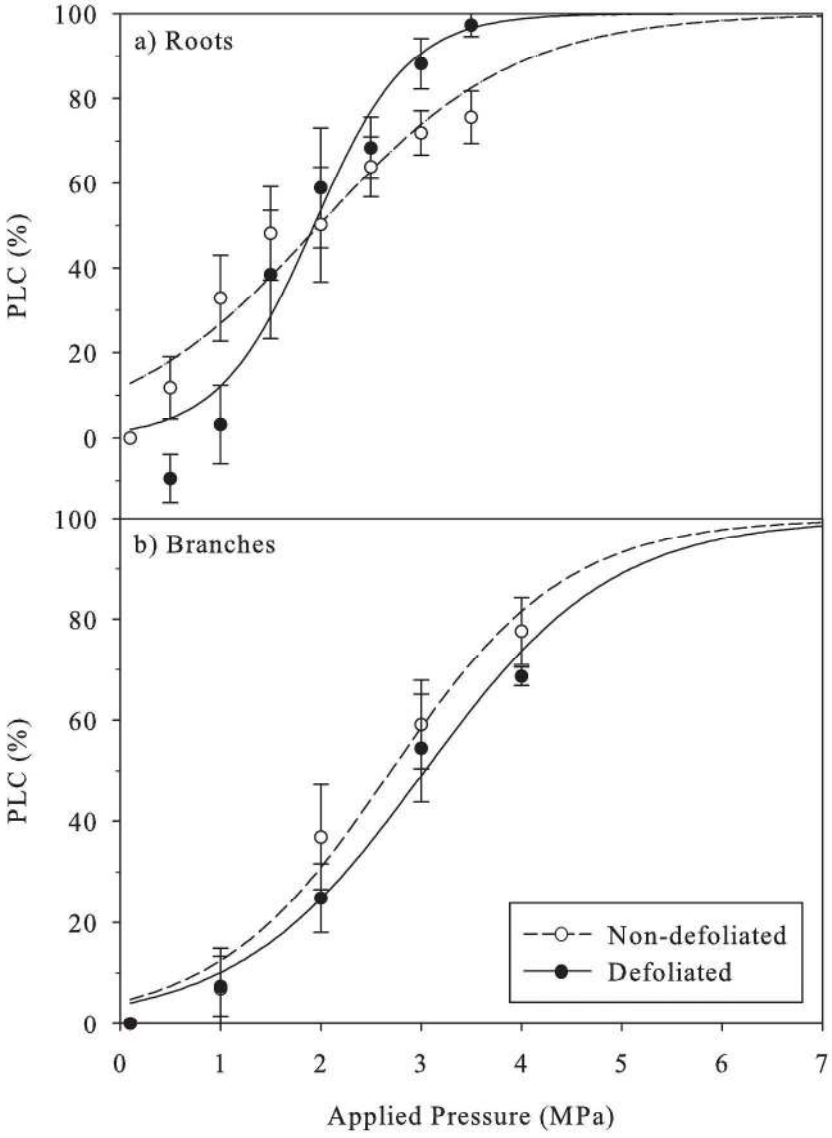


233x323mm (300 x 300 DPI)

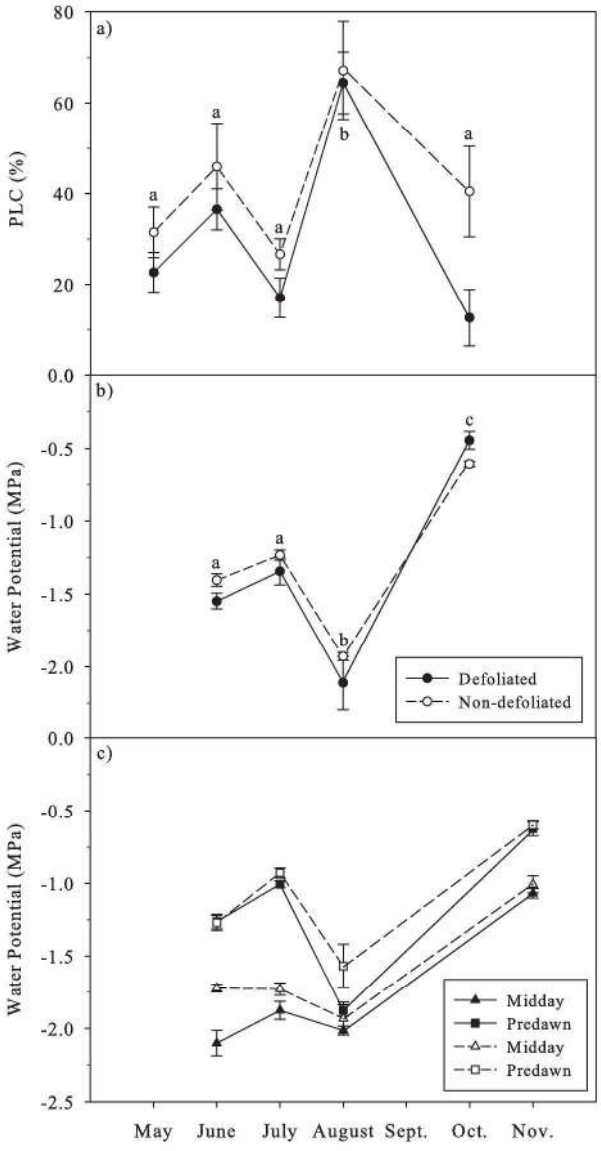


233x449mm (300 x 300 DPI)

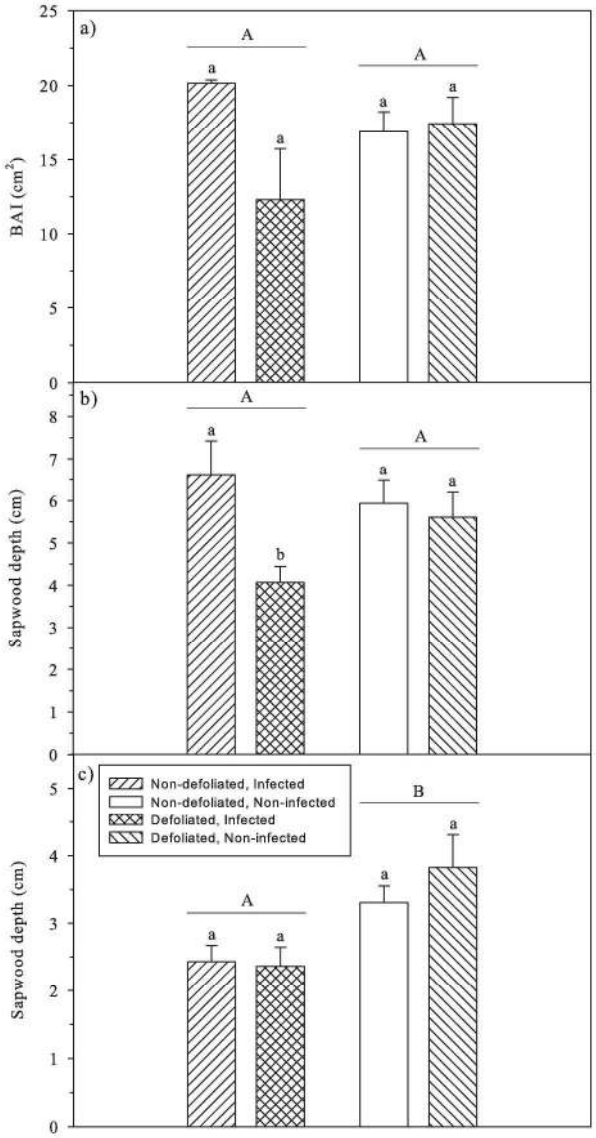


233x453mm (300 x 300 DPI)

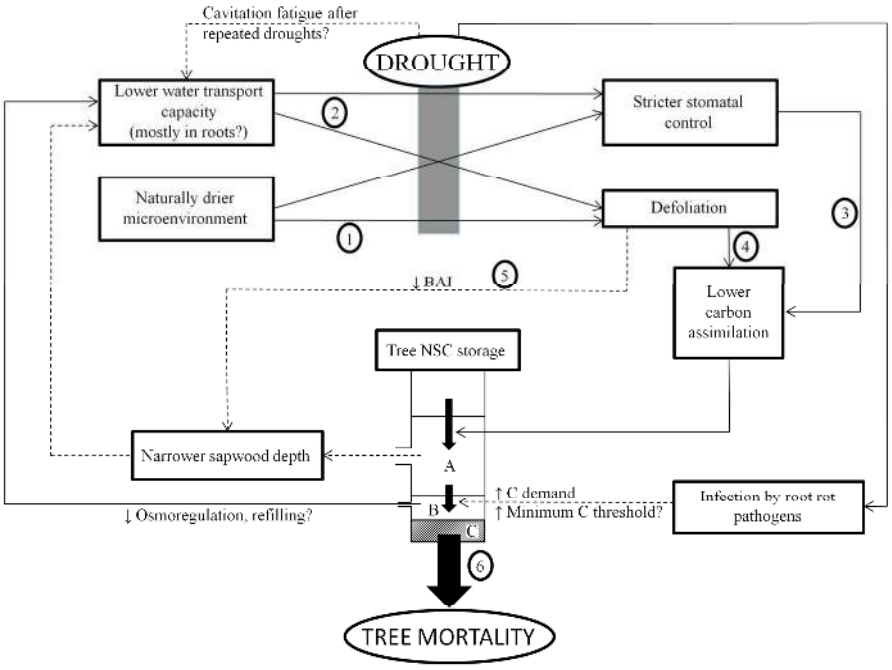


190x142mm (300 x 300 DPI)

# Tables

Table 1. Summary of the fitted linear mixed models with total non-structural carbohydrates (TNSC), the ratio between soluble sugars and total non-structural carbohydrates (SS:TNSC) and root starch as response variables. For factors, the coefficients indicate the difference between each level of a given variable and its reference level. In models the reference organ was "Leaves" (except in root starch where the effect of organ is not evaluated in the model), the reference month was "March", the reference defoliation class was "Defoliated" and the reference infestation occurrence was "Infected". The values are the estimate ± SE. Abbreviations: (ns) = no significant differences; • 0.05< *P*< 0.1; * 0.01< *P*< 0.05; ** 0.001< *P*< 0.01; *** *P*<0.001; ne = not evaluated in the model. Conditional $R^2$ values are given for each model.

| **Parameter** | **log(TNSC)** $R^2 = 0.90$ | **SS:TNSC** $R^2 = 0.61$ | **sqrt(Starch)** $R^2 = 0.57$ |
|---|---|---|---|
| Intercept | 2.50 ± 0.19*** | 0.54 ± 0.06*** | 0.65 ± 0.13*** |
| Branches | -1.31 ± 0.19*** | 0.27 ± 0.07*** | ne |
| Trunk | -3.22 ± 0.19*** | 0.10 ± 0.07 (ns) | ne |
| Roots | -2.78 ± 0.19*** | 0.07 ± 0.07 (ns) | ne |
| June | -0.15 ± 0.19 (ns) | -0.08 ± 0.07(ns) | -0.02 ± 0.18(ns) |
| August | -1.17 ± 0.19*** | 0.41 ± 0.07*** | -0.40 ± 0.18* |
| October | -1.28 ± 0.19*** | 0.37 ± 0.07*** | -0.51 ± 0.18** |
| Non-defoliated | 0.15 ± 0.17 (ns) | -0.10 ± 0.05• | 0.21 ± 0.21 |
| Non-infected | 0.18 ± 0.20 (ns) | -0.09 ± 0.06 (ns) | -0.17 ± 0.16 (ns) |
| Branches:June | 0.31 ± 0.19 (ns) | -0.13 ± 0.07• | ne |
| Trunk:June | 0.31 ± 0.19 (ns) | -0.03 ± 0.07 (ns) | ne |
| Roots:June | 0.21 ± 0.19 (ns) | 0.01 ± 0.07 (ns) | ne |

| | | | |
|---|---|---|---|
| Branches:August | 1.23 ± 0.19*** | -0.37 ± 0.08*** | ne |
| Trunk:August | 1.21 ± 0.19*** | -0.26 ± 0.08*** | ne |
| Roots:August | 1.26 ± 0.19*** | -0.23 ± 0.08** | ne |
| Branches:October | 0.88 ± 0.19*** | -0.35 ± 0.08*** | ne |
| Trunk:October | 1.26 ± 0.19*** | -0.33 ± 0.08*** | ne |
| Roots:October | 0.90 ± 0.19*** | -0.33 ± 0.08*** | ne |
| Branches:Non-defoliated | 0.05 ± 0.14 (ns) | 0.10 ± 0.05• | ne |
| Trunk:Non-defoliated | 0.05 ± 0.14 (ns) | 0.02 ± 0.05 (ns) | ne |
| Roots:Non-defoliated | 0.29 ± 0.14* | 0.04 ± 0.05 (ns) | ne |
| Branches:Non-infected | -0.28 ± 0.16• | 0.04 ± 0.06 (ns) | ne |
| Trunk:Non-infected | -0.36 ± 0.16* | 0.03 ± 0.06 (ns) | ne |
| Roots:Non-infected | -0.39 ± 0.16* | 0.03 ± 0.06 (ns) | ne |
| June:Non-defoliated | 0.31 ± 0.14* | -0.07 ± 0.05 (ns) | 0.28 ± 0.29 (ns) |
| August:Non-defoliated | 0.14 ± 0.14 (ns) | 0.11 ± 0.05* | 0.04 ± 0.29 (ns) |
| October:Non-defoliated | 0.27 ± 0.14 (ns) | 0.01 ± 0.05 (ns) | 0.47 ± 0.29 (ns) |
| June:Non-infected | 0.04 ± 0.16 (ns) | 0.05 ± 0.06 (ns) | 0.15 ± 0.22 (ns) |
| August:Non-infected | -0.10 ± 0.16* | 0.12 ± 0.06• | 0.14 ± 0.22 (ns) |
| October:Non-infected | 0.16 ± 0.16 (ns) | 0.07 ± 0.06 (ns) | 0.59 ± 0.22** |
| Non-defoliated:Non-infected | ne | ne | 0 ± 0.24 (ns) |
| June:Non-defoliated:Non-infected | ne | ne | -0.22 ± 0.33 (ns) |
| August:Non-defoliated:Non-infected | ne | ne | -0.13 ± 0.33 (ns) |
| October:Non-defoliated:Non-infected | ne | ne | -0.72 ± 0.33* |

12

Table 2. Summary of the fitted models with the vulnerability-curves parameters ($a$ and $P_{50}$), specific hydraulic conductivity ($K_S$), leaf specific conductivity ($K_L$) and leaf-to-sapwood area ratio ($A_L$:$A_S$) as response variables. In the models the reference organ was "Branches", the reference defoliation class was "Defoliated" and the infestation occurrence was "Infected". The values are the estimate ± SE. Abbreviations: (ns) = no significant differences; • 0.05 < $P$ < 0.1; * 0.01 < $P$ < 0.05; *** P < 0.001; ne = not evaluated in the model. Conditional $R^2$ values are given for each model.

| **Parameter** | **Parameter *a*** $R^2$ **= 0.37** | $P_{50}$ $R^2$ **= 0.40** | **log(*K*$_S$)** $R^2$ **= 0.10** | **log(*K*$_L$)** $R^2$ **= 0.36** | **log (A$_L$:A$_S$)** $R^2$ **= 0.11** |
|---|---|---|---|---|---|
| Intercept | -2.04 ± 1.38 (ns) | 2.72 ± 0.42*** | -8.70 ± 0.81*** | -16.56 ± 0.75*** | 7.48 ± 0.64*** |
| Roots | -1.80 ± 1.78 (ns) | -0.99 ± 0.55 (ns) | 0.20 ± 1.04 (ns) | ne | ne |
| Non-defoliated | -0.12 ± 1.20 (ns) | -0.51 ± 0.37 (ns) | 0.01 ± 0.70 (ns) | 1.90 ± 1.30 (ns) | -0.73 ± 1.10 (ns) |
| Non-infected | 0.36 ± 1.50 (ns) | 0.41 ± 0.46 (ns) | 1.12 ± 0.88 (ns) | 2.50 ± 0.89* | -0.83 ± 0.75 (ns) |
| Roots:Non-defoliated | 4.26 ± 1.74* | 0.42 ± 0.54 (ns) | 0.16 ± 1.02 (ns) | ne | ne |
| Roots:Non-infected | -2.74 ± 1.99 (ns) | -0.12 ± 0.61 (ns) | -0.67 ± 1.16 (ns) | ne | ne |
| Non-defoliated:Non-infected | ne | ne | ne | -2.71 ± 1.44• | 1.29 ± 1.22 (ns) |

Table 3. Summary of the fitted linear mixed models with the percentage loss of conductivity (PLC) and the water potential as response variables. The reference month was "May" in PLC and "June" in Water Potential, the reference defoliation class was "Defoliated" and the infestation occurrence was "Infected". The values are the estimate ± SE. Abbreviations: (ns) = no significant differences; • $0.05 < P < 0.1$; * $0.01 < P < 0.05$; ** $0.001 < P < 0.01$; *** P < 0.001; ne = not evaluated in the model. Conditional $R^2$ values are given for each model.

| **Parameter** | **PLC** **R2 = 0.45** | **Water Potential** **R2 = 0.82** |
|---|---|---|
| Intercept | 23.01 ± 10.98* | -1.57 ± 0.13*** |
| June | 10.95 ± 14.96 (ns) | ne |
| July | -9.95 ± 14.96 (ns) | -0.04 ± 0.19 (ns) |
| August | 45.23 ± 14.96** | -0.69 ± 0.19*** |
| October | -12.74 ± 15.00 (ns) | 1.14 ± 0.19*** |
| Non-defoliated | 8.60 ± 10.47 (ns) | 0.14 ± 0.13 (ns) |
| Non-infected | -0.52 ± 11.87 (ns) | 0.02 ± 0.15 (ns) |
| June:Non-defoliated | 0.25 ± 14.33 (ns) | ne |
| July:Non-defoliated | 0.19 ± 14.33 (ns) | -0.07 ± 0.18 (ns) |
| August:Non-defoliated | -5.15 ± 14.33 (ns) | 0.01 ± 0.18 (ns) |
| October:Non-defoliated | 14.72 ± 14.64 (ns) | -0.30 ± 0.19 (ns) |
| June:Non-infected | 4.42 ± 16.23 (ns) | ne |
| July:Non-infected | 6.51 ± 16.23 (ns) | 0.37 ± 0.21• |
| August:Non-infected | -5.16 ± 16.23 (ns) | 0.20 ± 0.21 (ns) |
| October:Non-infected | 9.13 ± 16.38 (ns) | -0.05 ± 0.21 (ns) |